Phase Field Simulation of Dendrite Growth of Fe-C Alloy in a Forced Flow

Xunfeng Yuan[1,a], Yan Yang[2,b]

[1]Department of Physics and Electronic Information Engineering, Shangluo University, Shangluo 726000, China

[2]Department of Mathematics and Computational Science, Shangluo University, Shangluo 726000, China

[a]yuanyang2011@163.com, [b]yanyangtianhao@163.com

Keywords: Phase-field method; Forced flow; Fe-C alloy; Isothermal solidification; Dendrite growth

Abstract. Based on the KKS model, the phase-field model is built by coupling with the concentration field and flow field, we simulate the dendrite growth during isothermal solidification of Fe-C alloy in a forced flow. The results show that the tip of dendrite arm is parabola shape, the secondary branch appear at the root of main branch, the dendrite growth presents obvious symmetry under the pure diffusion conditions. Because of fluid flushing, the solute concentration of the upstream dendrite arm is low, which lead to the dendrite grow fastly, thus the developed side-branch structure is formed, the tip velocity at steady state increased about 22.05% compared with the case without flow. Solute accumulate in the downstream of dendrite, which hindered the side-dendrite appear, the tip velocity at steady state decreased about 46.49% compared with the case without flow. The horizontal preferred direction of the dendrite is changed by fluid flow, hence horizontal main stem tilts towards the upstream direction.

Introduction

Dendrite is a common pattern during melt solidification, which determines the mechanical properties of cast materials. The existence of convection in solidification processes will remarkably alter the dendrite growth dynamics and lead to form different dendrite microstructure. Therefore, further study of dendrite growth under forced flow is an important theoretical and practical problem.

The phase field method is known to be very powerful in describing the complex pattern evolution of dendrite growth. The answer of the phase-field model equation can describe the condition, shapes and movement of the solid-liquid interface[1]. In the past couple of decades, the phase field method was orignally proposed for simulating dendrite growth in undercooled pure melts[2-4] and has been exrended to solidifiaction of alloys[5-12]. Ode[13] simulated isothermal dendrite growth and particle /interface interaction for Fe-C alloys. Suzuki[14] mainly considered the effect of the ternary alloying element on dendrite growth for Fe-C-P alloys. Oguchi[15] investigated the dendrite growth of Fe-C alloy using three different phase field models. Zhang[16] studied the influence of parameters on morphology and solute distribution of dendrite growth for Fe-C alloys . However, these simulations are focus on the pure diffusion conditions without considering the impact of liquid metal flow, dendrite growth in the flow is still lack of research until now.

In this paper, the phase-field model is built by coupling with the concentration field and flow field. The dendrite growth during isothermal solidification of Fe-C alloy in a forced flow is simulated, the morphologies, solute distributions, growth behaviors of tip on the dendrite growth are studied in detail.

Phase field model

In phase field model, a new important variable f (x,y,t), which characterizes the physical state of the system at each position in space and time was introduced. In this paper, f =1 means the bulk is solid phase and f =0 means the bulk is liquid phase. The solid-liquid interface is expressed by the steep layer

Published by Atlantis Press, Paris, France.

of f connecting the value 0 and 1. The phase field, solute concentration field, mass conservation and momentum equations are given, respectively, by

$$\frac{\partial f}{\partial t} = M[\nabla e^2(q)\nabla f - \frac{RT}{V_m}\ln\frac{(1-x_S^e)(1-x_L)}{(1-x_L^e)(1-x_S)} - Wg'(f)] \tag{1}$$

$$\frac{\partial x}{\partial t} + \nabla\cdot[\frac{x(1-f)}{1-f+k^e f}\vec{V}] = \nabla\cdot[D(f)\nabla x] + \nabla[D(f)h'(f)(x_L - x_S)\nabla f] \tag{2}$$

$$\nabla\cdot[(1-f)\vec{V}] = 0 \tag{3}$$

$$\frac{\partial}{\partial t}[(1-f)\vec{V}] + \nabla\cdot[(1-f)\vec{V}\cdot\vec{V}] = -(1-f)r/\nabla P + \nabla\cdot[u\nabla(1-f)\vec{V}] + \vec{M}_l^d \tag{4}$$

where R is gas constant, T temperature, V_m is molar volume, $D(f)=D_L+h(f)(D_S-D_L)$ is solute diffusion coefficient, and x is solute concentration of alloy, the subscripts S and L show solid and liquid phase, respectively. $\vec{M}_l^d = -2u(1+f)^2 f h\vec{V}/e^2$ is the dissipative interfacial stress, in which the constant h is 2.757. t is time, r, P and $\vec{V}$ are the density, pressure and flow velocity, respectively.

The phase-field parameters of e and W are related to interface energy s, and Interface width $2l$, and the parameters M is related to the kinetic coefficient m_k. The $g(f)$ and $h(f)$ are potential function. They are given by

$$e = \sqrt{\frac{6l}{2.2}s},\ W = \frac{6.6s}{l},\ M^{-1} = \frac{e^2}{s}(\frac{RT}{V_m}\cdot\frac{1-k^e}{m^e m_k} + \frac{e}{D_L\sqrt{2W}}\cdot\frac{RT}{V_m}(x_L^e - x_S^e)^2) \tag{5}$$

$$h(f) = f^3(10-15f+6f^2),\ g(f) = f^2(1-f)^2 \tag{6}$$

where m^e is equilibrium slope of liquidus, k^e equilibrium partition coefficient.

The four-hold anisotropy was introduced by putting the coefficient in the phase-filed parameter as follows

$$e(q) = e[1+e_4\cos(4q)] \tag{7}$$

where e_4 is the magnitude of anisotropy and $q = \arctan(f_Y/f_X)$ the angle between the normal direction of the interface and the X-axis. The effects of pressure are negligible for this work.

Numerical Simulations

In this article, Fe-0.5%C is chosen as the research object, and the physical property parameters in the calculation are easily obtained[16]: T_m=1810K, x_0=0.5% (mole fraction), s =0.204J/m^2, u =4.5×10^{-3} m^2/s, D_L =2.0×10^{-8}m^2/s, D_S =6.0×10^{-9}m^2/s, k^e =0.204, $l = 3\Delta X$, m^e =-1836K/mol, ΔT =27K, V_m =7.7×10^{-6}m^3/mol, e_4 =0.02.

An initial crystal is in a pure undercooled melt and its radius is assumed to be R_0. The melt enters the domain from the top. The initial conditions are given by

$$\begin{cases}(X-500)^2+(Y-500)^2 < R_0^2 & (f=1, V_X=0, V_Y=0, x=x_0)\\ (X-500)^2+(Y-500)^2 \geq R_0^2 & (f=1, V_X=0, V_Y=\mathrm{U}, x=x_0)\end{cases} \tag{8}$$

where X is (100) direction and Y is (010) direction. In the calculation of the regional border, Zero-Neumann boundary condition is chosen in the phase filed and concentration field.

For the numerical calculation, Eqns.(1)-(4) are made discrete on the uniform grids using explicit finite difference methods. The space steps ΔX and time steps Δt should comply with $\Delta X \leq l$ and $\Delta t \leq (\Delta X)^2/4D_L$ respectively. The grid area is 1000×1000, time steps Δt =1×10^{-9}s, space steps $\Delta X = \Delta Y$ =1×10^{-8}m.

Results and Discussion

Morphology of dendrite growth. Figure 1 shows the phase field morphology of isothermal solidification dendrite growth for U=0 and 0.05m/s, respectively. It can be seen that in the case of without flow, the dendrite grows symmetrically in four preferentially growing directions, the tip of dendrite arm was parabola shape and the secondary branch appear at the root of main branch. Based on the observations of length of main branch, we find that the dendrite length along the X, Y axis positive direction slightly less than it along the negative direction, because of calculation errors.

In the case of forced flow, dendrite shows asymmetry in four growing directions. The dendrite arm grow fastest in upstream and slowest in the downstream, and the velocity of dendrite arm at horizontal direction is somewhere in between. Compared with the case of without flow, the length of the upstream and the horizontal dendrite arms increased about 20.50%, 0.33% respectively. But the length of the downstream dendrite arms decreased about 39.71%. Side-branches are formed at the upstream of the horizontal principal branch, the gap of secondary branch is small, develops the integration growth, but no side-branches appear on longitudinal principal branch. The preferred growth direction of horizontal dendrite is changed, which make the horizontal main branch tilts towards the upstream direction, the tilt angle of the horizontal main branch of the X-axis positive direction and negative direction are 3.74 ° and 3.56 ° respectively.

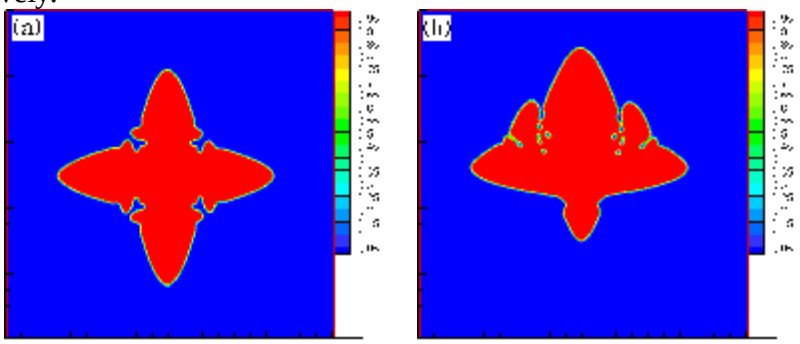

Fig1 The phase field morphology of isothermal solidification dendrite growth: (a) without flow (b) forced flow

Solute distribution of dendrite growth. Figure 2 shows the solute distribution of isothermal solidification dendrite growth corresponds to phase field morphology in Figure 1. It can be seen from Fig.2(a) that under pure diffusion conditions, the solute diffusion layer around the dendrite tip is thin, the solute diffuse timely, leading to the dendrite grows rapidly. Furthermore, in the root of main branch between the dendrite arms, the solute diffuse difficultly, which leading to the dendrite grows slowly. From Fig.2(b), it can be found that because of fluid flushing, the solute concentration of the upstream dendrite arm is low, the actual supercooling of it is great, which lead to the dendrite grow fastly, thus the developed side-branch structure is formed. Solute accumulate in the downstream, the concentration of the downstream dendrite arm is high, the actual supercooling of it is small, which hindered the side-dendrite appear.

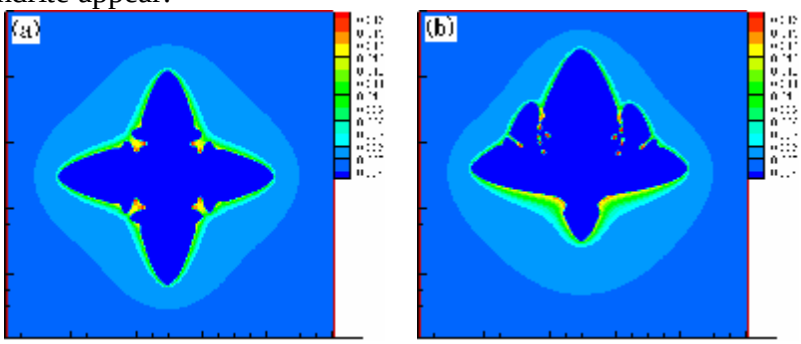

Fig.2 The solute distribution of isothermal solidification dendrite growth: (a) without flow (b) forced flow

The growth behavior of the dendrite tip. In order to further grasp the growth law of dendrite tip in a forced flow, the effect of forced flow on the dendrite tip growth behavior are analysised

quantitatively. The calculated dendrite tip velocity, tip radius and tip solute concentration at various time compared with the results under pure diffusion conditions is demonstrated in Fig.3. Due to calculation errors, the dendrite arm growth of the Y-axis positive and negative direction is different, the dendrite arm tip data of Y-axis positive and negative direction are calculated separately under pure diffusion conditions.

From the figure it can be seen that in the initial stage of solidification, dendrite tip velocity and tip radius gradually decreases, but tip solute concentration increases, this is because initial undercooling drive the rapid growth of dendrites. With the conduct of solidification process, the rejected solute accumulates at the interface, making the undercooling decreases, the dendrite growth velocity decreases. Meanwhile, because of fluid flushing, a large number of solute from the upstream side to the downstream side, which leading to the solute accumulates seriously in downstream side, undercooling reduces fast and the growth rate changes rapidly. After a transient period, the data of different tips reach approximately stable values with different levels, indicating that the solute rejection has been balanced by the solute diffusion and flow. Compared with the pure diffusion, the upstream tip velocity and tip radius at steady state increases by about 22.05% and 43.92%, respectively. The downstream tip velocity and tip radius at steady state decreases by about 46.49% and 21.46%, respectively. The upstream tip solute concentration at steady state decreases by about 4.05%. The downstream tip solute concentration at steady state increases by about 10.68%.

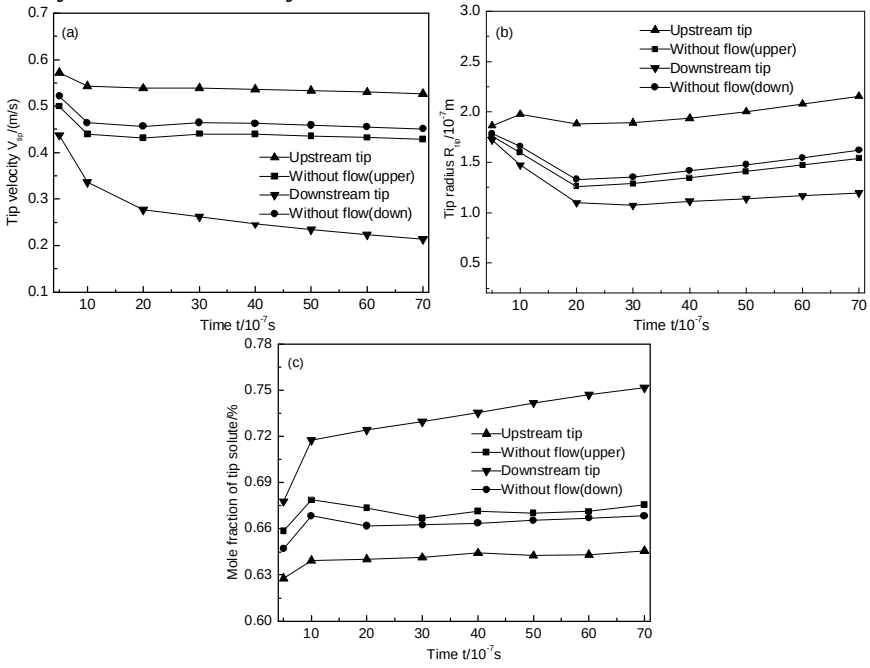

Fig.3 Time histories of tip velocity(a),tip radius(b) and tip solute concentration(c) for the case of dendrite arm growth

Conclusions

Under the pure diffusion conditions, the tip of dendrite arm is parabola shape, the secondary branch appears at the root of main branch, the dendrite morphology and solute distribution presents obvious symmetry. Under flow velocity is equal to 0.05m/s, dendrite shows asymmetry in four growing directions. The upstream dendrite arm grows fastest whose length increased about 20.50% and the downstream dendrite arm grows slowest whose length decreased about 39.71%. Meanwhile, horizontal main branch tilts towards the upstream direction, the tilt angle of the horizontal main branch of the X-axis positive direction and negative direction are 3.74 ° and 3.56 °, respectively. When the solute rejection has been balanced by the solute diffusion and flow, the upstream tip velocity at steady state increased about 22.05% compared with the case without flow, the downstream tip velocity at steady state decreased about 46.49% compared with the case without flow.

Published by Atlantis Press, Paris, France.

Acknowledgements

This work was supported by the Doctoral Fund of Shangluo University (NO. 12SKY01-1).

References

[1] A. A. Wheeler, W. J. Boettinger and G. B. Mcfadden: Phy. Rev. E, Vol. 45 (1992), No.10 p.7424.

[2] A. Karma and W J Rappel: Phys. Rev. E, Vol. 57 (1998), No. 4 p. 4323.

[3] X. Tong, C. Beckermann and A. Karma: Phys Rev E, Vol. 61 (2000), No. 1 p. 49.

[4] Y.T. Ding, X.F. Yuan and Y. Hu: Acta Metall. Sin. (Engl. Lett.), Vol. 23 (2010), No. 2 p. 121.

[5] A. Drevermann, L. Sturz and N. Warnken: Mater. Sci. Eng. A, Vol. 413-414 (2005), p. 259.

[6] W.Y. Long, D.L. Lu, C. Xia, M.M. Pan, C.Q. Cai and L.L. Chen: Acta Phys Sin., Vol. 58 (2009), No. 11 p.7802.

[7] Q. Sun, Y.T. Zhang, H.X. Cui and C.Z. Wang: China foundry, Vol. 5 (2008), No. 4 p. 265.

[8] Y.T. Zhang, C.Z. Wang, D. Z. Li and Y.Y. Li: Acta Metall. Sin. (Engl. Lett.), Vol. 22 (2009), No. 3 p. 197.

[9] J.W. Wang, Z.P. Wang, Y. Lu, C.S. Zhu, L. Feng and R.Z. Xiao: Trans. Nonferrous Met. Soc. China, Vol. 22 (2012), No. 2 p. 391.

[10] X.F. Yuan, Y.T. Ding, T.B. Guo and Y. Hu: The Chinese Journal of Nonferrous Metal, Vol. 20 (2010), No. 4 p. 681.

[11] J.J. Li, J.C. Wang and G.C. Yang: Chin. Phys. B, Vol. 17 (2008), No. 9 p. 3516.

[12] X.F. Yuan, Y.T. Ding, T.B. Guo and Y. Hu: The Chinese Journal of Nonferrous Metal, Vol. 20 (2010), No. 8 p. 1474.

[13] M. Ode, T. Suzuki, S.G. Kim and W.T. Kim: Sci. Technol. Adv. Mater., Vol. 1 (2000), No. 1 p. 43.

[14] T.Suzuki, M. Ode, S.G. Kim and W.T. Kim : J. Cryst. Growth, Vol. 237 (2002), No. 1-2 p. 125.

[15] K. Oguchi and T.Suzuki: ISIJ International, Vol. 49 (2009), No. 10 p. 1536.

[16] Y.T. Zhang, D.H. Li, C. Z. Wang and Y.Y.Li: Chinese Journal of Materials Research, Vol. 23 (2009), No. 3 p. 317.